RESEARCH PAPER

Photosynthesis in C_3–C_4 intermediate *Moricandia* species

Urte Schlüter[1], Andrea Bräutigam[1,3], Udo Gowik[2], Michael Melzer[4], Pascal-Antoine Christin[5],
Samantha Kurz[1], Tabea Mettler-Altmann[1] and Andreas PM Weber[1,*]

[1] Institute of Plant Biochemistry, Cluster of Excellence on Plant Sciences (CEPLAS), Heinrich Heine University, Universitätsstr. 1, 40225 Düsseldorf, Germany

[2] Institute of Plant Molecular and Developmental Biology, Cluster of Excellence on Plant Sciences (CEPLAS), Heinrich Heine University, Universitätsstr. 1, 40225 Düsseldorf, Germany

[3] Network Analysis and Modelling, Leibniz Institute of Plant Genetics and Crop Research (IPK), OT Gatersleben, Corrensstr. 3, 06466 Stadt Seeland, Germany

[4] Structural Cell Biology, Leibniz Institute of Plant Genetics and Crop Research (IPK), OT Gatersleben, Corrensstr. 3, 06466 Stadt Seeland, Germany

[5] Department of Animal and Plant Sciences, University of Sheffield, Western Bank, Sheffield S10 2TN, UK

* Correspondence: Andreas.Weber@uni-duesseldorf.de

Abstract

Evolution of C_4 photosynthesis is not distributed evenly in the plant kingdom. Particularly interesting is the situation in the Brassicaceae, because the family contains no C_4 species, but several C_3–C_4 intermediates, mainly in the genus *Moricandia*. Investigation of leaf anatomy, gas exchange parameters, the metabolome, and the transcriptome of two C_3–C_4 intermediate *Moricandia* species, *M. arvensis* and *M. suffruticosa*, and their close C_3 relative *M. moricandioides* enabled us to unravel the specific C_3–C_4 characteristics in these *Moricandia* lines. Reduced CO_2 compensation points in these lines were accompanied by anatomical adjustments, such as centripetal concentration of organelles in the bundle sheath, and metabolic adjustments, such as the balancing of C and N metabolism between mesophyll and bundle sheath cells by multiple pathways. Evolution from C_3 to C_3–C_4 intermediacy was probably facilitated first by loss of one copy of the glycine decarboxylase P-protein, followed by dominant activity of a bundle sheath-specific element in its promoter. In contrast to recent models, installation of the C_3–C_4 pathway was not accompanied by enhanced activity of the C_4 cycle. Our results indicate that metabolic limitations connected to N metabolism or anatomical limitations connected to vein density could have constrained evolution of C_4 in *Moricandia*.

Key words: Bundle sheath, C_3–C_4 intermediacy, C_4 photosynthesis, evolution, glycine decarboxylase, *Moricandia*.

Introduction

C_4 plants evolved in warm, open, and often arid regions, where the C_4 concentrating mechanism leads to enhanced photosynthetic carbon fixation efficiency (Sage, 2004). In most C_4 species, this is achieved by upstream CO_2 fixation through phospho*enol*pyruvate carboxylase (PEPC) in the mesophyll (MS) and transport of the synthesised C_4 metabolites to the bundle sheath (BS) cells (Hatch, 1987). Decarboxylation of C_4 metabolites in the BS cells increases CO_2 concentration around Ribulose-1,5 bisphosphate carboxylase/oxygenase (Rubisco), thus promoting the carboxylase reaction while reducing photorespiration (Hatch and Slack, 1970; Bowes *et al.*, 1971; Hatch, 1987). Division of photosynthetic

biochemistry between two different cell types requires anatomical adaptation including high vein density, reduction of MS tissue, and enlarged, chloroplast-rich BS cells (Dengler *et al.*, 1994; McKown and Dengler, 2007; Christin *et al.*, 2013). Despite its complexity, the C_4 trait evolved independently more than 60 times in flowering plants (Sage *et al.*, 2012; Sage, 2016). Soon after the discovery of C_4 photosynthesis, it became apparent that transition from C_3 to C_4 photosynthesis could not have been realised in one giant step, but more likely evolved via a series of transitory states (Kennedy and Laetsch, 1974). Potential C_3–C_4 intermediates were identified by their CO_2 compensation point, which lay between the values of C_3 and C_4 species, as well as some C_4-like anatomical features in the BS cells (Kennedy and Laetsch, 1974; Krenzer *et al.*, 1975). The Brassicaceae species *Moricandia arvensis* was among the first species classified as a potential C_3–C_4 intermediate (Krenzer *et al.*, 1975).

The genus *Moricandia* consists of eight accepted species (www.theplantlist.org), all originating from Mediterranean or Saharo-Sindian areas (Tahir and Watts, 2010). Based on CO_2 compensation points, *Moricandia* includes C_3 species (*M. moricandioides*, *M. foetida*, and *M. foleyi*) as well as C_3–C_4 intermediates (*M. arvensis*, *M. suffruticosa*, *M. nitens*, *M. spinosa*, and *M. sinaica*; Brown and Hattersley, 1989; Apel *et al.*, 1997). Besides a low CO_2 compensation point, the C_3–C_4 candidates exhibit lower sensitivity to O_2 (Holaday *et al.*, 1982) and high incorporation of ^{14}C into glycine and serine (Holaday and Chollet, 1983; Hunt *et al.*, 1987). The BS area per cell profile is increased as well as the number of chloroplasts, mitochondria, and peroxisomes in the BS (Holaday and Chollet, 1983; Hunt *et al.*, 1987). In contrast to C_4 species, these potential intermediates possess a C_3-like $\delta^{13}C$ signature, C_3-like Rubisco kinetics (Bauwe and Apel, 1979; Holbrook *et al.*, 1985), and low activities of typical C_4 enzymes such as PEPC, pyruvate phosphate dikinase (PPDK), NADP malic enzyme (NADP-ME), NAD-ME, and phospho*enol*pyruvate carboxykinase (PEPCK) (Holaday *et al.*, 1981; Holaday and Chollet, 1983).

Rawsthorne and colleagues showed that the P-subunit of the glycine decarboxylase multi-enzyme system (GLDP) is exclusively localised to the BS of the leaf of *M. arvensis* (Rawsthorne *et al.*, 1988*a, b*; Rylott *et al.*, 1998), while all other enzymes of the photorespiratory or photosynthetic pathways, such as the L, H, and T subunits of GLD, serine hydroxymethyltransferase (SHMT), glycolate oxidase (GOX), and Rubisco, are found in MS as well as BS tissues (Rawsthorne *et al.*, 1988*b*, Morgan *et al.*, 1993). These findings led to the first experimentally verified model of photosynthesis in C_3–C_4 intermediates (Rawsthorne, 1992). The interruption of the photorespiratory cycle in the MS caused by the absence of the functioning GLD/SHMT complex leads to an accumulation of glycine and its diffusion to the BS cells. There, its decarboxylation creates a local CO_2 enrichment, thus increasing the carboxylation activity of Rubisco in the BS and therefore reducing the CO_2 compensation point of the leaf (Rawsthorne, 1992). This process is also named the glycine shuttle, photorespiratory CO_2 pump, or C_2 photosynthesis (Sage *et al.*, 2014).

Species with C_3–C_4 intermediate characteristics have been identified in diverse groups of plants (Krenzer *et al.*, 1975; Rajendrudu *et al.*, 1986; Moore *et al.*, 1987; Hylton *et al.*, 1988; Apel *et al.*, 1997; Muhaidat *et al.*, 2011; Sage *et al.*, 2011*b*; Wen and Zhang, 2015; Khoshravesh *et al.*, 2016). Phylogenetic studies have shown that many of these C_3–C_4 plants are closely related to C_4 siblings, and it is therefore likely that intermediates served as transitory states on the evolutionary path from C_3 to C_4 (McKown *et al.*, 2005; Christin *et al.*, 2011*a*; Fisher *et al.*, 2015; Lyu *et al.*, 2015). The possibility that C_3–C_4 intermediates bridge the evolutionary gap between C_3 and C_4 states has also recently been supported by different computational modelling approaches (Heckmann *et al.*, 2013; Williams *et al.*, 2013; Mallmann *et al.*, 2014; Brautigam and Gowik, 2016). Experimental as well as computational models predict that under favourable genetic and anatomic pre-conditions, the shift of GLD to the BS is a decisive step for installation of the glycine shuttle and the transition from C_3 to C_3–C_4 photosynthesis. Because the GLD/SHMT reaction in the BS releases not only CO_2 but also NH_3, rebalancing of the N metabolism between the two cell types is required (Mallmann *et al.*, 2014). For re-balancing of N metabolism, the current model suggests additional metabolite shuttles, e.g. glutamate–2-oxoglutarate, alanine–pyruvate, and aspartate–malate. Parts of these shuttles and the associated biochemical enzymes also play an important role in C_4 photosynthesis. Existing C_4 enzymes and transporters can create a primordial C_4 cycle in the C_3–C_4 background on which selection can act as long as selective pressure for efficient C assimilation persists (Aubry *et al.*, 2011; Mallmann *et al.*, 2014; Brautigam and Gowik, 2016). In essence, altered GLD localisation is predicted to initiate a smooth path to C_4 (Heckmann *et al.*, 2013; Brautigam and Gowik, 2016; Schluter and Weber, 2016). In support of this model, over 90% of plant lineages with C_3–C_4 intermediates also contain C_4 species (Mallmann *et al.*, 2014).

The model, however, fails to explain the presence of evolutionary stable C_3–C_4 intermediates. The situation in the Brassicaceae is therefore particularly interesting; to date no *sensu stricto* C_4 species have been identified in this family, but it contains multiple lines of C_3–C_4 intermediates, including members of the genus *Moricandia* (Hylton *et al.*, 1988), *Diplotaxis tenuifolia* (Apel *et al.*, 1997; Ueno *et al.*, 2006), and *Brassica gravinae* (Ueno, 2011). In this current study, the C_3–C_4 metabolism in the genus *Moricandia* was investigated in more detail by simultaneous analyses of phylogeny, leaf anatomy, gas exchange, and metabolite and transcript patterns in closely related C_3 (*M. moricandioides*) and C_3–C_4 species (*M. arvensis* line MOR1 and *M. suffruticosa*). The data were used for testing hypotheses related to C_4 evolution or lack thereof: (i) phylogenetic patterns of GLDP explain the evolution of intermediacy in just one specific branch of the Brassicaceae; (ii) metabolic differences between C_3 and intermediate species relate to the N-shuttle; and (iii) differences with the genus *Flaveria*, which evolved full C_4, indicate where *Moricandia* species might be restricted in evolution towards C_4.

Material and methods

Plant cultivation

Seeds for different *Moricandia* lines were obtained from botanic gardens and seed collections (*Moricandia moricandioides*, 04-0393-10-00 from Osnabrück Botanic Gardens; *M. arvensis*, line 12-0020-10-00 from Osnabrück Botanic Gardens, lines 0119708, 0000321, 0084187 from the Royal Botanic Gardens in Kew, lines MOR1 and MOR3 from IPK Gatersleben; *M. suffruticosa*, line 0105433 from the Royal Botanic Gardens in Kew; *M. nitens*, 0209858 from the Royal Botanic Gardens in Kew). Seeds were vapour-sterilised by incubation in a desiccator together with a freshly prepared mix of 100 ml 13% Na-hypochloride with 3 ml of 37% HCl for 2 h. The sterilised seeds were then germinated on plates containing 0.22% (w/v) Murashige Skoog medium, 50 mM MES pH 5.7 and 0.8% (w/v) Agar. After about a week, seedlings were transferred to pots containing a mixture of sand and soil (BP substrate, Klasmann & Deilmann GmbH, Germany) at a ratio of 1:2. In the first experiment, testing all the *Moricandia* lines, plants were grown in a greenhouse (Heinrich Heine University, Düsseldorf) in September 2013, where they received natural light ranging from 300 and 600 µmol s⁻¹ m⁻². For our more detailed studies of C₃–C₄ intermediate metabolism in *Moricandia*, we chose one species from each *Moricandia* C₃–C₄ subgroup presented in Fig. 1A (*M. suffruticosa* from group I and *M. arvensis* line MOR1 from group II) and compared them to their C₃ relative *M. moricandioides*. For all following experiments, plants

were cultivated in a climate chamber (CLF Mobilux Growbanks, Wertingen, Germany) under 12-h day conditions with 23/20 °C day/night temperatures. The plants were exposed to ambient CO_2 concentrations and irradiance at plant level was ~200 µmol s⁻¹ m⁻². All experiments were conducted before the transition to the reproductive state. Mature leaf material was harvested from *M. moricandioides*, *M. arvensis* (line MOR1), and *M. suffruticosa* ~2 h after the start of the light period by flash-freezing in liquid nitrogen. The material was homogenised into a fine powder by grinding in liquid nitrogen. The material was stored at –80 °C and used for analysis of elements, metabolites, transcripts, and proteins.

Phylogeny

Relationships between *Moricandia* species and their closest relatives were determined using sequences from the ITS nuclear region. DNA was extracted from all the *Moricandia* lines available in our study, *Diplotaxis tenuifolia* (line 'Wilde Rauke', origin: N.L. Chrestensen Erfurter Samen-und Pflanzenzucht GmbH), and *D. viminea* (line GB.31066, origin: Rijk Zwaan Distribution B.V., Netherlands). The ITS sequences were amplified and sequenced using the primers ITS1 (O'Kane *et al.*, 1996) and ITS4 (White *et al.*, 1990). Additional ITS sequences were retrieved from the NCBI database (see Supplementary Table S1 at *JXB* online). The sequences were aligned with Muscle (Edgar, 2004), and the alignment was used to infer a time-calibrated phylogeny following a relaxed molecular clock
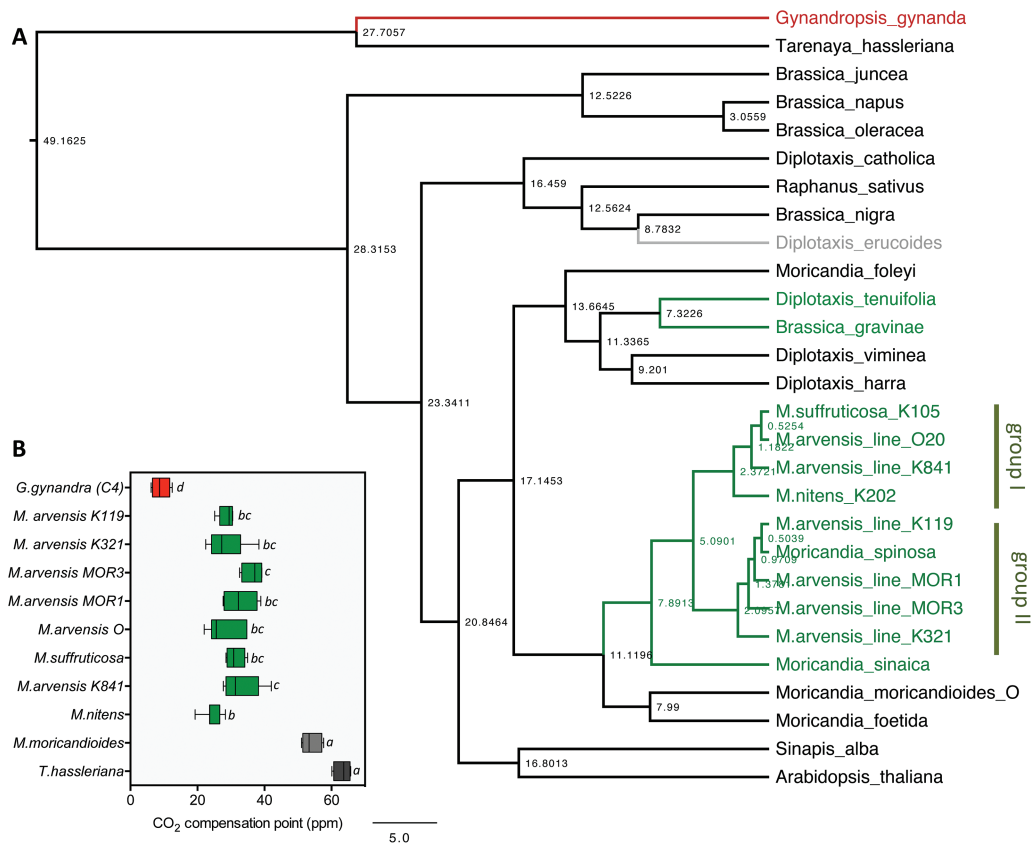

Fig. 1. C₃-C₄ intermediate species in the Brassicaceae. (A) Time-calibrated phylogeny of the Brassicaceae species selected for this study. The *Moricandia* species build one branch of the tree with an early separation of the C₃ species *M. moricandioides* and *M. foetida*, and the C₃–C₄ intermediate species *M. suffruticosa*, *M spinosa*, *M. sinaica*, *M. nitens*, and different *M. arvensis* lines. Additional independently established C₃–C₄ intermediate species are *Diplotaxis tenuifolia* and *Brassica gravinae*. The closest C₄ relative *G. gynandra* belongs to the Cleomaceae. C₃ species are in black; C₃–C₄ intermediate species in green, with gray for the potential intermediate *D. erucoides*; C₄ species in red. The scale bar is 5 Ma. (B) CO₂ compensation points determined from A-C_i curves in C₃ and C₃–C₄ *Moricandia* lines compared with C₃ and C₄ species from the Cleomaceae. Significant differences were determined by ANOVA followed by Tukey's HSD multiple comparison test with alpha ≤0.01.

approach, as implemented in Beast (Drummond and Rambaut, 2007). The analysis was run for 10 000 000 generations, sampling a tree every 1000 generations under a GTR+G+I substitution model, a log-normal relaxed clock, and a Yule speciation prior. The tree was rooted by forcing the monophyly of both the outgroup (the two '*Cleome*' species) and the ingroup (Brassicaceae). The tree was calibrated by setting the age of the crown of Brassicaceae with a normal distribution with a mean of 29.3 Ma and a standard deviation of 3.0, based on estimates from markers across nuclear genomes (Christin *et al.*, 2014). The convergence of the analysis and adequacy of the burn-in period were verified using Tracer (Drummond and Rambaut, 2007). Medians of node ages for tree samples after a burn-in period of 1 000 000 generations were mapped on the maximum-credibility tree using Treeannotator (Drummond and Rambaut, 2007).

GLDP-specific mRNA sequences were retrieved from online databases (see Supplementary Table S2). GLDP-specific coding sequences for *Moricandia* and *Diplotaxis* lines were obtained from the assembly of next-generation sequencing reads produced in our own lab (see below). The phylogenetic tree was constructed with the help of the Phylogeny.fr webtool (http://phylogeny.lirmm.fr) in the default mode consisting of alignment by Muscle, G-block building, maximum-likelihood tree generation by PhyML, and visualisation by TreeDyn.

Plant anatomy

Vein density measurements were done on the top third of fully grown rosette leaves. The leaf material was cleared in an acetic acid:ethanol mix (1:3) overnight followed by staining of cell walls in 5% safranin O in ethanol, and de-staining in 70% ethanol. Pictures were taken using a Nikon Eclipse Ti-U microscope equipped with a ProgRes MF camera (Jenoptik, Jena, Germany), at 4× magnification. At least six leaves were analysed for vein density per line, always with five pictures measured and averaged per leaf using ImageJ open software (https://imagej.nih.gov/ij/).

For histological and ultrastructural analysis 2-mm^2 sections from mature rosette leaves were used for combined conventional and microwave-proceeded fixation, dehydration, and resin embedding in a PELCO BioWave®34700-230 (Ted Pella, Inc., Redding CA, USA) as described in Supplementary Table S3. Semi-thin sections with a thickness of approximately 2.5 μm were mounted on slides and stained for 2 min with 1 % methylene blue / 1% Azur II in 1% aqueous borax at 60 °C prior to light microscopical examination in a Zeiss Axio Imager M2 microscope (Carl Zeiss Microscopy GmbH, Göttingen, Germany). Ultra-thin sections with a thickness of approximately 70 nm were cut with a diamond knife, transferred onto TEM-grids and contrasted in a LEICA EM STAIN (Leica Microsystems, Vienna, Austria) with uranyl acetate and Reynolds' lead citrate prior to analysis using a Tecnai Sphera G2 transmission electron microscope (FEI, Eindhoven, Netherlands) at 120 kV.

Photosynthetic gas exchange

Mature rosette leaves were used for gas exchange measurements with a LICOR 6400XT (LI-COR Biosciences, Lincoln, USA). The settings were a flow of 300 μmol s^{-1}, light of 1500 μmol m^{-2} s^{-1}, leaf temperature of 25 °C, and the vapour pressure deficit was kept below 1.5 kPa. Initial analysis of the *Moricandia* lines and comparison with the related C$_3$ plants *Brassica oleraceae* and *Tarenaya hassleriana*, the C$_3$–C$_4$ intermediate *Diplotaxis tenuifolia*, and the C$_4$ plant *Gynandropsis gynandra* were done with A-C_i curves, with measurments at 400, 50 100, 200, 400, 800, 1200, and 1800 ppm CO$_2$. Significance of the differences in the CO$_2$ compensation points

between lines was tested using a one-way ANOVA followed by a post-hoc Tukey's multiple comparison test.

More detailed A-C_i curves were measured on the selected species *M. moricandioides*, *M. arvensis* MOR1, and *M. suffruticosa*. After acclimation, an A-C_i curve was determined starting at a CO$_2$ concentration (C_a) of 400 ppm, then going down to 20 ppm in nine steps, then going back to 400 ppm and raising the CO$_2$ concentration stepwise up to 1800 ppm. Measurements at the lowest six CO$_2$ concentrations were used to extract the CO$_2$ compensation point and the initial slope of the graph corresponding to the carboxylation efficiency. Maximal assimilation was determined at CO$_2$ concentrations of 1600 to 1800 ppm. At least six plants were measured per line, and statistical significance between values for the different species was evaluated using Student's t-test.

Metabolite and element analysis

The homogenized leaf material was extracted for metabolite analysis by gas chromatography-mass spectrometry (GC-MS) according to Fiehn *et al.* (2000) using a 7200 GC-QTOF (Agilent, Santa Clara, USA). Data analysis was conducted with the Mass Hunter Software (Agilent, Santa Clara, USA). For relative quantification, all metabolite peak areas were normalized to the peak area of an internal standard of ribitol added prior to extraction. The same homogenised leaf material was used for determination of δ^{13}C and CN ratios. After lyophilisation, the material was analysed using an Isoprime 100 isotope ratio mass spectrometer coupled to an ISOTOPE cube elemental analyzer (both from Elementar, Hanau, Germany) according to Gowik *et al.* (2011). Measurements were always done on ten biological replicates. Statistical significance was analysed using Student's t-test.

Transcript analysis

Total RNA was extracted from the homogenized leaf material using the GeneMatrix Universal RNA purification kit (Roboklon GmbH, Berlin, Germany). The RNA was treated with DNase for a few seconds only and quality controlled on a Bioanalyzer 2100 (Agilent, Santa Clara, USA). Subsequently, mRNA purification and adapter ligation was performed with the TruSeq RNA Sample Preparation Kit (Illumina, San Diego, USA) using 1 μg of total RNA. After a second quality control on the Bioanalyzer, samples were sent to Beckmann Coulters Genomics (Danvers, MA, USA) and sequenced on a HiSeq2500 sequencer (Illumina, San Diego, CA) as single-end 100-bp reads. Three to four biological replicates were used per *Moricandia* species with between 13 and 17 million reads per sample. The reads were aligned to a minimal set of coding sequences of the TAIR 10 release of the Arabidopsis genome (http://www.arabidopsis.org/) using BLAT (Kent, 2002) in protein space. The best BLAT hit for each read was determined by (1) the lowest *e*-value and (2) the highest bit score (Brautigam *et al.*, 2011). Raw read counts were transformed to reads per million (rpm) to normalize for the number of reads available at each sampling stage. Cross-species mapping takes advantage of the completeness and annotation of the Arabidopsis genome. In all samples, 80 to 86% of reads mapped to the reference genome. Comparison of the transcript pattern between species was performed with the edgeR tool (Robinson *et al.*, 2010) in R (www.R-project.org) using the Benjamini–Hochberg false discovery test with a cut-off at false discovery rate (FDR) ≤0.01 for significant differences. The agriGO webtool was employed for gene ontology (GO) term analysis (Du *et al.*, 2010). The transcriptome data was deposited at the GEO repository (www.ncbi.nlm.nih.gov/geo/) under the accession number GSE87343.

For construction of the specific *Moricandia* transcript assemblies, one sample per line was sequenced as pair-end 150-bp reads on an Illumina HiSeq2000 platform at the BMFZ (Biologisch-Medizinisches Forschungszentrum) of the Heinrich Heine University (Düsseldorf, Germany). The resulting reads were trimmed using the trimmomatic tool (Bolger *et al.*, 2014) followed by assembly using Trinity (Haas *et al.*, 2013), which yielded between 68 000 and 91 000 contigs. Sequences for transcripts from *D. tenuifolia*, *D. viminea*, and *D. muralis* were obtained following the same protocol.

PEPC activity

Total soluble proteins were extracted from the homogenised leaf material in 50 mM Hepes-KOH pH 7.5, 5 mM MgCl$_2$, 2 mM DTT, 1 mM EDTA, 0.5% Triton-X-100, 0.1% ß-mercaptoethanol. For the PEPC assay, 20 µl of the extract were mixed with assay buffer consisting of 100 mM Tricine-KOH pH 8.0, 5 mM MgCl$_2$, 2 mM DTT, 1 mM KHCO$_3$, 0.2 mM NADH, 5 mM glucose-6-phosphate, 2 U ml^{-1} malate dehydrogenase in a microtiter plate (Ashton *et al.*, 1990). The reaction was started after addition of phospho*enol*pyruvate to a final concentration of 5 mM in the assay. Absorbance at 340 nm was measured with a Synergy HT microplate reader (BioTek Instruments, USA). Protein content of the solutions was determined with the Bradford assay (Quick Start Bradford Protein Assay kit, BioRad). The ratio between fresh and dry weight of the leaf material was determined by weighing a second mature leaf from the same plants before and after drying it at 70 °C overnight.

Results

Occurrence of C$_3$–C$_4$ intermediates in the Brassicaceae

The phylogenetic relationships between all the *Moricandia* accessions available in our study were investigated by sequencing their ITS region and in comparison with data available in the NCBI database (Fig. 1A). We aimed at testing whether the C$_3$–C$_4$ character evolved independently or in one single event in different *Moricandia* lines. With the exception of *M. foleyi*, all *Moricandia* species formed a monophyletic group in the phylogenetic tree (Fig. 1A). Within this clade, a C$_3$ group (*M. moricandioides*, *M. foetida*) was sister to the C$_3$–C$_4$ intermediate species (*M. arvensis*, *M. suffruticosa*, *M. nitens*, *M. sinaica*, *M. spinosa*; Fig. 1A), indicating that the evolution of the C$_3$–C$_4$ intermediate character is most-parsimoniously explained by a single event in the *Moricandia* genus. Intermediates with smaller, more ellipse-shaped leaves (group I, Fig. 1A; Supplementary Fig. S1) formed a monophyletic group, while the intermediates with mainly longer petioles formed a paraphyletic clade (group II). Lines taxonomically assigned to *M. arvensis* could be found within both groups.

Besides the *Moricandia* C$_3$–C$_4$ species, very similar features, such as significantly reduced CO$_2$ compensation points, occur in *Diplotaxis tenuifolia* and *Brassica gravinae* (Apel *et al.*, 1997; Ueno, 2003, 2011). The development of C$_3$–C$_4$ intermediacy in these species was clearly independent from the events in *Moricandia* (Fig. 1A). Phylogenetic trees of the Brassicaceae with higher species density (Warwick and Sauder, 2005; Arias *et al.*, 2014) suggest that these species belong to different

branches of the tree and that C$_3$–C$_4$ intermediacy also evolved independently in *D. tenuifolia* and *B. gravinea*. In the list of Apel *et al.* (1997), single measurements of CO$_2$ compensation points in *D. muralis* and *D. erucoides* also indicated low CO$_2$ compensation points. *Diplotaxis muralis* is a hybrid between *D. viminea* (C$_3$) and *D. tenuifolia* (C$_3$–C$_4$) and usually closer to C$_3$ in its gas exchange characteristics (Ueno *et al.*, 2006), but detailed studies are lacking for *D. erucoides*. It is also remarkable that C$_3$–C$_4$ intermediates were only found in the Oleracea group of the Brassiceae tribe, in the lineage II Brassicaceae (Apel *et al.*, 1997; Warwick and Sauder, 2005; Arias *et al.*, 2014), but no C$_3$–C$_4$ intermediates have so far been identified in any other subgroup of this large family.

Physiological features allow differentiation of C$_3$ and C$_3$–C$_4$ Moricandia lines

Many details of the C$_3$–C$_4$ intermediate photosynthesis character were investigated in the 1980s and 1990s at the University of Nebraska (see Holaday *et al.*, 1981, 1982; Holaday and Chollet, 1983), in Gatersleben in Germany (see Bauwe and Apel, 1979; Apel *et al.*, 1997), and at the John Innes Centre in Norwich, UK (see Rawsthorne *et al.*, 1988*a*, *b*; Rylott *et al.*, 1998). Since the stock seed material from these initial analyses could no longer be obtained, CO$_2$ compensation points in genotyped greenhouse-grown lines were characterized (Fig. 1B) and compared with data from the C$_3$ plant *T. hassleriana* and the C$_4$ plant *G. gynandra* from the neighbouring Cleomaceae family. The measurements of the CO$_2$ compensation points clearly allowed classification of the tested lines as a C$_3$, C$_3$–C$_4$, or C$_4$ species (Fig. 1B). All C$_3$–C$_4$ intermediate lines had CO$_2$ compensation points that were significantly lower than in the C$_3$ species, but also significantly higher than in the C$_4$. On the other hand, no significant differences could be observed among the C$_3$–C$_4$ intermediate lines.

The selected accessions *M. moricandioides*, *M. arvensis* MOR1, and *M. suffruticosa* were then grown under controlled environmental conditions in a climate chamber. Under these conditions, the differences in the CO$_2$ compensation point of the C$_3$ and C$_3$–C$_4$ *Moricandia* species were even more pronounced (Fig. 2A, B). A closer inspection of the shape of *A*-*C*$_i$ curves showed that, despite the low CO$_2$ compensation point, the curve of the intermediates looked much more similar to the C$_3$ curve than the one of the C$_4$ species *G. gynandra*, which had a very steep initial $\Delta A / \Delta C_i$ slope of 0.557 (Fig. 2A). The initial slope of the *A*-*C*$_i$ curve is connected to the carboxylation efficiency in the photosynthetic system, the PEPC efficiency in C$_4$, and the Rubisco carboxylation efficiency in C$_3$ (von Caemmerer, 2000). A comparison of the *A*-*C*$_i$ curves in the C$_3$ and C$_3$–C$_4$ *Moricandia*s showed that the initial slope was actually steeper in the C$_3$ species than in the C$_3$–C$_4$ intermediate lines (Fig. 2A, C).

The assimilation at ambient CO$_2$ was lower in the C$_3$–C$_4$ intermediate species than in the C$_3$ species (Fig. 2D). Differences in conductance were not responsible for this variation, and the maximal CO$_2$ assimilation at high CO$_2$ reached similar levels in all species tested (see Supplementary Table S4). In addition, measurements of PEPC activity in extracts

from mature leaves indicated that PEPC did not play a major role in the primary fixation of CO_2 in C_3–C_4 intermediate *Moricandia* species (Fig. 2G). No significant differences could be observed in the carbon isotope ratio of the C_3 and C_3–C_4 intermediate species (Fig. 2E). The protein content per total dry weight tended to be lower in the intermediates as compared to the related C_3 species *M. moricandioides*; however, these results were only significant for one C_3–C_4 line, *M. arvensis* (Fig. 2F).

Differences in CO_2 compensation points are connected to anatomical changes

The development of C_3–C_4 intermediate physiology relies on functional specification of metabolism in the MS and BS cells and an increase in the metabolite exchange between the two cell types. Differences among photosynthetic types were therefore expected to be closely connected to changes in the anatomy, which were evaluated on a histological and ultrastructural level.

Measurements of vein length per area revealed that the C_3–C_4 *Moricandia* species had lower or equal vein density when compared to the C_3 relative (Fig. 2H). In the top view of cleared leaves, veins of C_3–C_4 intermediate species appeared thicker than in the C_3 species (Fig. 3A–C), probably connected to the large number of chloroplasts, which were centripetally arranged around the veins in the leaf cross-sections (Fig. 3D–I). In-depth ultrastructural analysis showed a high number of mitochondria located predominantly in the cytoplasm between the chloroplasts and the cell wall of adjacent cells of the vascular tissue of C_3–C_4 plants (Fig. 3J–L). The C_3 species *M. moricandioides* had eight cell layers, while
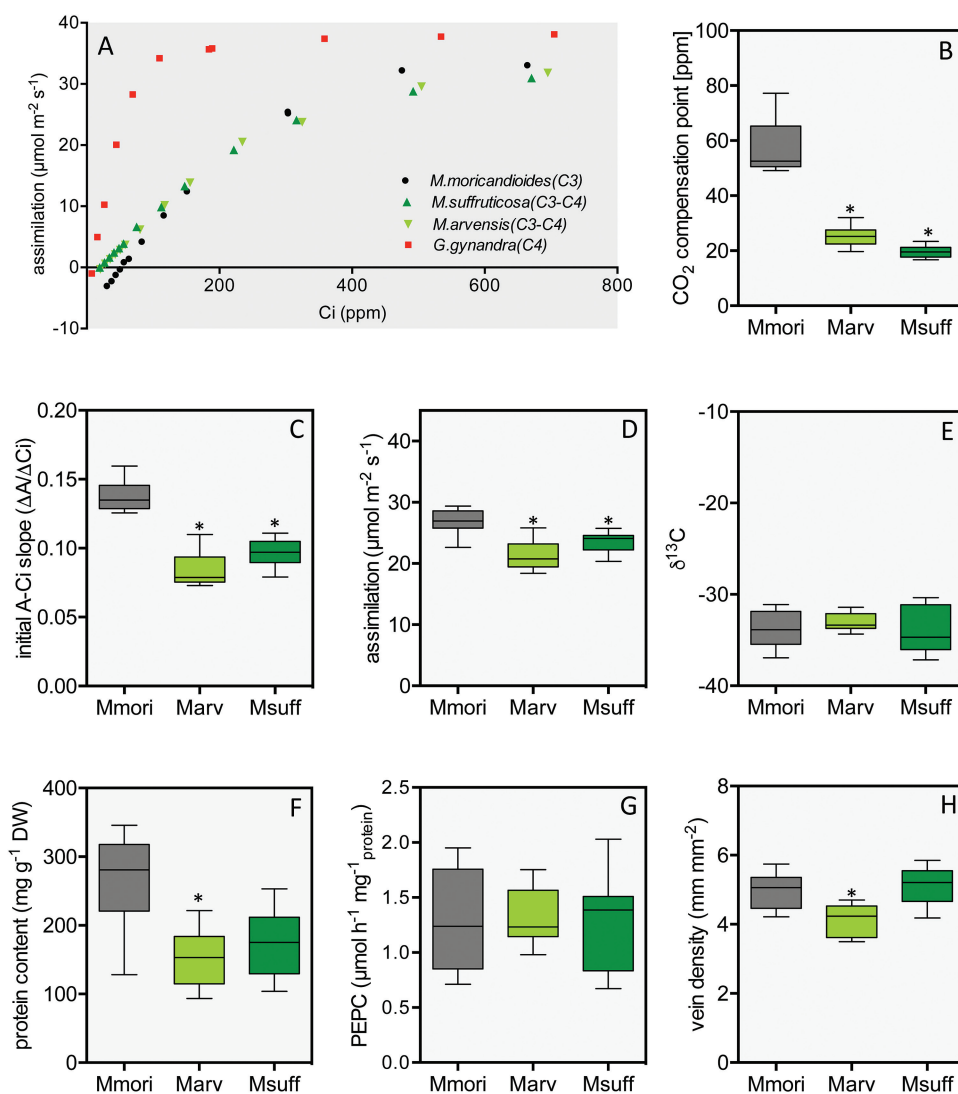

Fig. 2. Physiological features in the C_3 species *M. moricandioides*, and the C_3–C_4 intermediate species *M. suffruticosa* and *M. arvensis* line MOR1. (A) Representative examples of A-C_i curves from *M. moricandioides*, *M. suffruticosa*, and *M. arvensis* line MOR1 in comparison with the curve from the C_4 species *G. gynandra*. (B) CO_2 compensation points; (C) initial A-C_i slope; (D) assimilation rate under ambient conditions with c_a of 400 ppm; (E) $δ^{13}C$ signature of leaf material; (F) protein content per plant dry weight; (G) PEPC activity; (H) vein density in the top part of mature leaves. All box-whisker plots show data summarised from 8–10 biological replicates. The asterisks indicate significant differences of the C_3–C_4 intermediate species in comparison with the C_3 species *M. moricandioides*, as determined by a *t*-test ($P≤0.01$). Mmori, *M. moricandioides*; Marv, *M. arvensis* line MOR1; Msuff, *M. suffruticosa*. (This figure is available in colour at *JXB* online.)
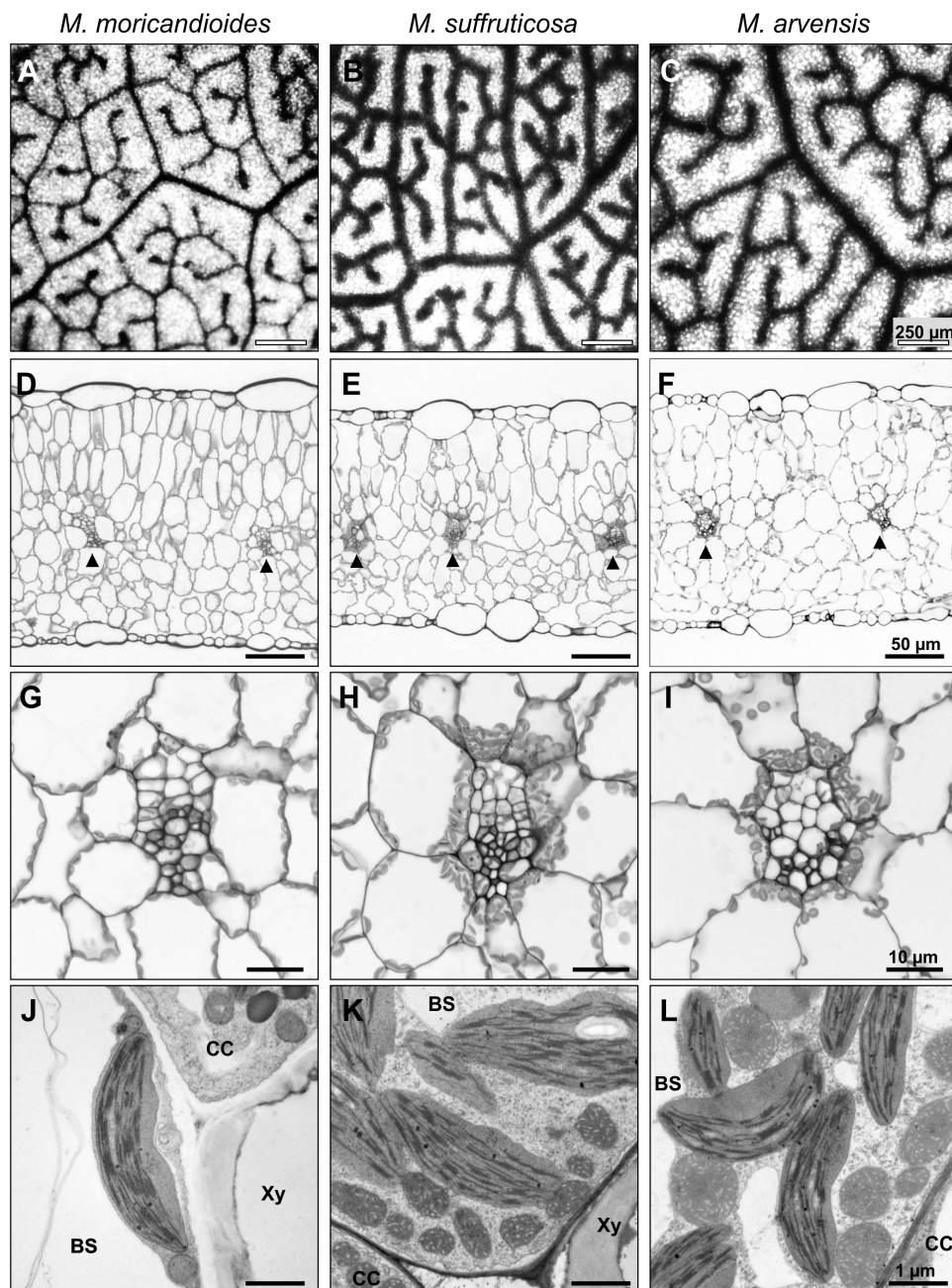
C_3–C_4 metabolism in intermediate *Moricandia* species | **197**

Fig. 3. Anatomy of the C_3 species *M. moricandioides* (A, D, G, J), and the C_3–C_4 intermediate species *M. suffruticosa* (B, E, H, K) and *M. arvensis* line MOR1 (C, F, I, L). (A–C) Top view of cleared leaves showing the general vein pattern; (D–F) overview of cross-sections; (G–I) close-up of the arrangement of chloroplasts in the bundle sheath cells; (J–L) transmission electron microscopy of bundle sheath cells with organelles arranged next to the vein cell. Arrow heads indicate vascular bundles. BS, bundle sheath cell; Xy, xylem cell; CC, companion cell.

M. suffruticosa and *M. arvensis* both had one MS cell layer fewer (Supplementary Table S4, Fig. 3D–F). Such a reduction in the MS tissue alone could be responsible for a shift in the leaf cell profile towards a higher proportion of BS cells (McKown and Dengler, 2007).

Specific metabolite pattern in C_3–C_4 intermediates

The metabolite pattern of the leaves is expected to be influenced by species-specific differences as well as by the photosynthesis type. The overall metabolite patterns in *M. moricandioides*, *M. suffruticosa*, and *M. arvensis* were first assessed by

principal component analysis (PCA) (see Supplementary Fig. S2A). In the first principal component (PC1), samples from the C_3 species *M. moricandioides* localised predominantly to the right, next to samples of C_3–C_4 intermediate species. PC2 mainly separated the two C_3–C_4 intermediate species. The samples from both C_3–C_4 intermediates were also characterised by high variation. Three metabolites showed significantly ($P \leq 0.01$) different concentrations in all tested comparisons (*M. arvensis* vs *M. moricandioides*, *M. suffruticosa* vs M. *moricandioides*, and *M. suffruticosa* vs *M. arvensis*): maleic acid, serine, and threonine (Supplementary Fig. S2B). To distinguish between C_3 and C_3–C_4 intermediate species, we screened

for metabolites that significantly differed between the C$_3$ and the two C$_3$–C$_4$ species, but not between the two intermediates. Among the nine metabolites in this category were alanine, glycine, GABA, gluconic acid, leucine, malate, malonic acid, and valine (Supplementary Fig. S2B, Supplementary Table S4).

The predicted N shuttle metabolites (Mallmann *et al.*, 2014), glutamate, alanine, and malate, had higher concentrations in both intermediate *Moricandia* lines. Aspartate was only increased in *M. suffruticosa* (Fig. 4). Glycolate and glycerate are part of the photorespiratory pathway, but no significant differences in the concentration of these two metabolites were detected in leaves of the C$_3$ and C$_3$–C$_4$ *Moricandia* species (Fig. 4), confirming that these metabolites do not play a major role in coordination of metabolism between MS and BS cells.

Transcript patterns do not show a strong specific C$_3$–C$_4$ signature

Next-generation sequencing allows an analysis and comparison of the transcriptomes of species for which no reference genome is available by mapping the reads against the minimal transcriptome of *Arabidopsis thaliana* (Brautigam *et al.*, 2011). In all *Moricandia* samples, between 79% and 86% reads were mapped, which is higher than in previous work with Asterales species (Gowik *et al.*, 2011). PCA showed that the transcript pattern was most prominently influenced by the species (see Supplementary Fig. S3A). PC1 clearly separated samples from *M. moricandioides*, *M. arvensis*, and *M. suffruticosa*, while PC2 only separated *M. moricandioides* and *M. arvensis* from *M. suffruticosa* (Supplementary Fig. S3A). Subsequent PCs were already influenced by replicate-specific differences. An influence of the photosynthesis type was not detected in the first three PCs (Supplementary Fig. S3B).

The abundance of 1671 transcripts was significantly different in the C$_3$ and the C$_3$–C$_4$ intermediate leaves, but not between the two intermediates. All of these had changed in both C$_3$–C$_4$ intermediate species to the same direction: 797 were commonly enhanced in C$_3$–C$_4$ while 874 were commonly reduced in C$_3$–C$_4$ (Supplementary Fig. S3C, Supplementary Table S5). GO term analysis of both groups of transcripts revealed quite diverse categories. Only two GO terms were enriched among transcripts enhanced in C$_3$–C$_4$, while 21 process GO-terms were enriched in transcripts reduced in C$_3$–C$_4$. The latter included high-level terms such as cellular compound, nitrogen metabolism, and carbohydrate metabolism. The cellular compartment mainly affected by transcript reduction in C$_3$–C$_4$ intermediates appeared to be the chloroplast (see Supplementary Table S6).

The metabolism in C$_3$–C$_4$ intermediate leaves is predicted to differ from C$_3$ leaves mainly with respect to cellular distribution of photorespiratory processes and subsequent re-adjustment of C and N balance by metabolite shuttle mechanisms (Mallmann *et al.*, 2014). Transcripts predicted to be involved in all these processes were therefore studied in more detail. No changes were observed for transcripts encoding components of the photorespiratory pathway, in particular the GLDP protein, which is only present in the BS
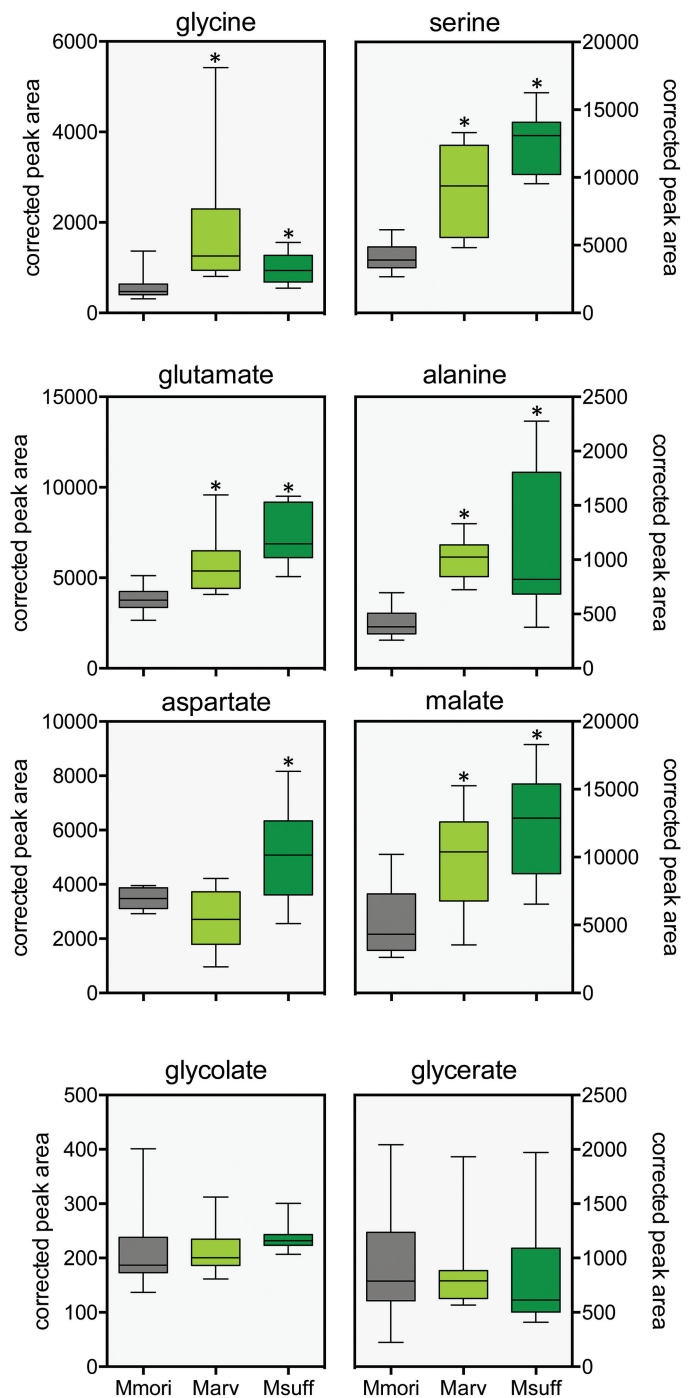

Fig. 4. Selected metabolites in the C$_3$ species *M. moricandioides*, and the C$_3$–C$_4$ intermediate species *M. suffruticosa* and *M. arvensis* line MOR1. The box-whisker plots represent summaries of 10–12 biological replicates. The asterisks indicate significant differences between the C$_3$–C$_4$ and the C$_3$ species as determined by a *t*-test ($P \leq 0.01$). Mmori, *M. moricandioides*; Marv, *M. arvensis* line MOR1; Msuff, *M. suffruticosa*. (This figure is available in colour at *JXB* online.)

cell of C$_3$–C$_4$ intermediates (Fig. 5). Not all transcripts of the Calvin–Benson–Bassham (CBB) cycle did show significant differences between C$_3$ and C$_3$–C$_4$ species. It was, however, noticeable that almost all transcripts tended to be reduced in the C$_3$–C$_4$ intermediate species when compared to C$_3$ (Fig. 5).

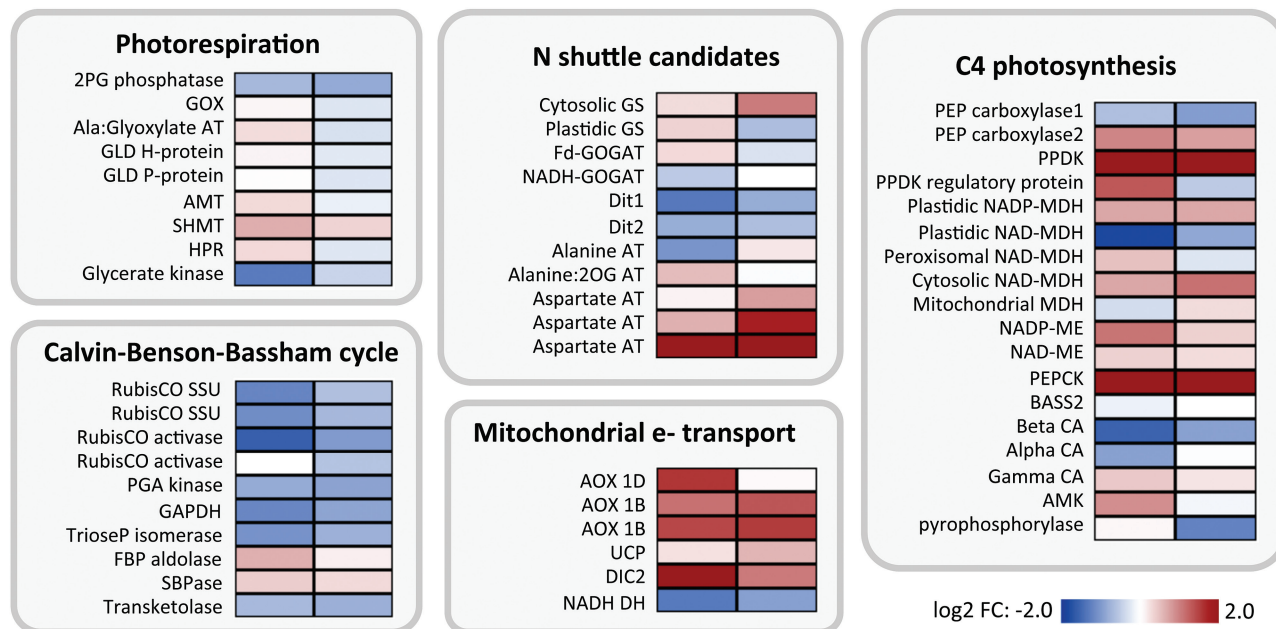Expression of transcripts belonging to the photorespiratory and CBB pathways is generally lower in C$_4$ than C$_3$ species

Fig. 5. Transcriptional changes in selected pathways. The heat maps indicate the log$_2$-fold changes in transcript level between C$_3$–C$_4$ species *M. arvensis* line MOR1 (left column) and *M. suffruticosa* (right column) and the C$_3$ species *M. moricandioides*. Blue indicates reduced transcript abundance in C$_3$–C$_4$, red indicates enhanced transcript abundance in C$_3$–C$_4$.

(Brautigam *et al.*, 2011). The evolutionary trajectory of pathway expression from C$_3$ via C$_3$–C$_4$ to C$_4$ metabolism can be followed in *Flaveria* species and compared to the results from *Moricandia*. No large changes in the average transcript abundance of the photorespiratory pathway were detected in the intermediate *Flaveria* species. The abundance of photorespiratory transcripts decreased only in the C$_4$-like *F. brownii* and then even more in the C$_4$ species (Fig. 6). The same pattern was also observed for the CBB cycle. A decrease of CBB cycle transcripts in intermediates without increased C$_4$ cycle activity, as we found in the two investigated *Moricandia* species, was not observed in *Flaveria* (Fig. 6).

Transcripts encoding enzymes with potential functions in the metabolite shuttles between MS and BS cells were inspected in detail. Only the aspartate aminotransferase (*AspAT*) encoding genes were enhanced in both intermediates compared to the C$_3$ species (Fig. 5). Furthermore, transcripts that could potentially be recruited into a C$_4$ cycle were tested for their pattern (Fig. 5). In *Flaveria*, basic C$_3$–C$_4$ intermediates were characterised by increases in alanine aminotransferase (*AlaAT*) and NADP-malic enzyme (*NADP-ME*) transcripts, in the evolutionary series this was followed by increases in *PEPC* transcripts, which were enhanced in all but one of the basic *Flaveria* intermediates (*F. chloraefolia*; Fig. 6). In C$_3$–C$_4$ intermediate *Moricandia* species, *AlaAT* transcripts were not enhanced, and only slight increases in *NADP-ME* transcripts were observed (Fig. 5). Another potential C$_4$ decarboxylating enzyme, *PEPCK*, showed enhanced transcript abundance in the C$_3$–C$_4$ *Moricandia* intermediates (Fig. 5; Supplementary Table S7). The same was true for the *PPDK* transcripts. Two *PEPC* transcripts with C$_3$-like characteristics (Paulus *et al.*, 2013) were found in noticeable amounts in *Moricandia* leaves. The higher-abundant form was actually reduced compared to the C$_3$ transcriptome, and only the lower-abundant form was

enhanced in the intermediates (Fig. 5; Supplementary Table S7).

The GLD/SHMT reaction in the BS also produces NADH and this may require adjustments of the redox balance in the cells. Strong increases were observed for transcripts encoding alternative oxidases (*AOX*) in the C$_3$–C$_4$ intermediates. The same tendency was found for the uncoupling protein (*UCP*) and the dicarboxylate transporter *DIC2* (see Supplementary Table S7). A NADH dehydrogenase transcript on the other hand was reduced in the C$_3$–C$_4$ leaves (Fig. 5). Increases in *AOX* and *UCP* transcripts were not unique to *Moricandia*, but were also observed in the C$_3$–C$_4$ *Flaveria* intermediates. In the C$_4$-like and C$_4$ *Flaveria* species, the *AOX* and *UCP* transcripts decreased again compared to the C$_3$ plant. Hence the increase in *AOX* transcript abundance was a common feature in C$_3$–C$_4$ intermediate *Moricandia* and *Flaveria* species (Figs 5 and 6).

Moricandia *species possess only a single copy of the* GLDP *gene*

The number of *GLDP* copies and their phylogenetic relationship was investigated in the Brassicaceae. Only species where full genome information was available were considered for the comparison. *Arabidopsis thaliana* has two copies of the gene, *AtGLDP1* and *AtGLDP2* (Engel *et al.*, 2007). Comparison with other Brassicaceae revealed that other species from the Brassicaceae lineage I (*Arabidopsis lyrata*, *Camalina sativa*, *Capsella rubella*) as well as species from the extended lineage II (*Eutrema salsugineum*, *Thellungiella halophila*) also possess transcripts with high similarity to both *Arabidopsis* genes (Fig. 7). From *Arabis alpina* only the *AtGLDP2*-like gene was identified. In the *Brassica* species *B. rapa*, *B. oleracea*, and *B. napus* on the
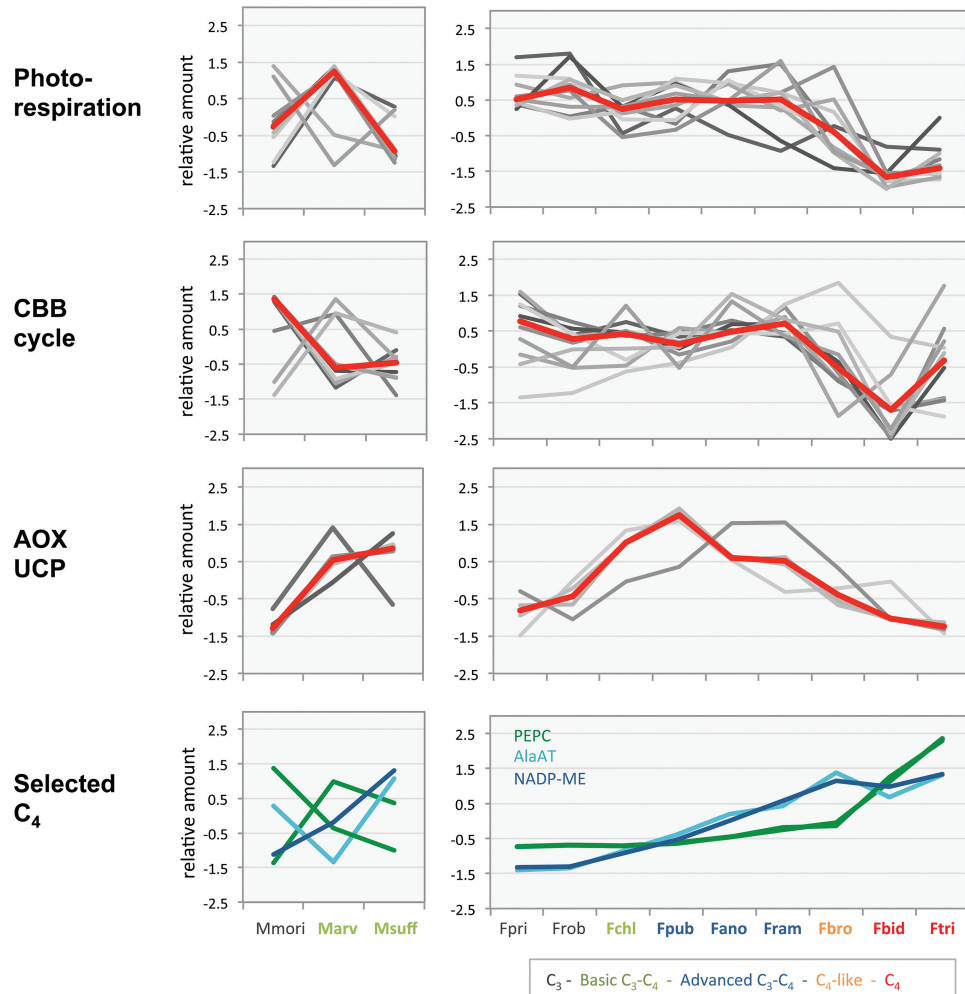
Fig. 6. Comparison of the changes in transcript levels of the *Moricandia* species and *Flaveria* species with different degrees of C₄ features. The graphs show the relative amount (*z*-score normalised data of mean rpm values) from transcripts belonging to the selected pathways. The general trend in the transcription pattern of a pathway is indicated in red as the median of the individual transcripts values. Species abbreviations are: Mmori, *M. moricandioides*; Marv, *M. arvensis*; Msuff, *M. suffruticosa*; Fpri, *F. pringlei*; Frob, *F. robusta*; Fchl, *F. chloraefolia*; Fpub, *F. pubescence*; Fano, *F. anomala*; Fram, *F. ramosissima*; Fbro, *F. brownii*; Fbid, *F. bidentis*; Ftri, *F. trinervia*.

other hand, only *AtGLDP1*-like copies were found (Fig. 7). Transcriptomes from mature leaves of *M. moricandioides*, *M. suffruticosa*, *M. arvensis*, *Dipoltaxis tenuifolia*, *D. viminea*, and *D. muralis* also assembled only copies with high similarity to the *AtGLDP1* gene. In all these species, *GLDP* was represented by one unique transcript. Two transcripts were assembled only in *D. muralis*, one with a high similarity to the sequence of *D. tenuifolia* and the other one with a high similarity to the *D. viminea* sequence. Since *D. muralis* is a hybrid between these two species, this was expected and underlines the successful assembly of the *GLDP* gene sequences in our study. An assembly of gene sequences from a leaf transcriptome could still miss copies that are simply not expressed at all in the leaves examined. The complete absence of *AtGLDP2*-like sequences also in the genome of the sequenced *Brassica* species, however, indicated that the *AtGLDP2* copy was absent in the whole Brassiceae subgroup containing *Brassica*, *Moricandia*, and *Diplotaxis* species, most likely by loss at the base of Brassiceae subgroup.

Discussion

Evolution from C₃ to C₃–C₄ was promoted by lack of a second GLDP *copy in the Brassiceae*

Evolution of C₄ photosynthesis is not equally distributed across the plant kingdom, being frequent in some groups but completely absent from many others with similar growth forms (Sage *et al.*, 2011a; Sage, 2016). In the Brassicaceae we find no true C₄, but possibly three independent C₃–C₄ lines (*Moricandia*, *Diplotaxis tenuifolia*, *Brassica gravinae*), and all these lines belong to the Oleracea group of the Brassiceae (Warwick and Sauder, 2005; Arias *et al.*, 2014).

The decisive step from C₃ to C₃–C₄ intermediacy is associated with a shift of the activity of photorespiratory GLD from ubiquitous expression to almost exclusive expression in the BS (Heckmann *et al.*, 2013; Khoshravesh *et al.*, 2016). Detailed studies of the promoter sequences of the GLDP in *Flaveria* have shown that the regulatory elements mediating BS-specific expression were already present in the C₃ ancestors (Schulze *et al.*, 2013). *Flaveria* species possess two
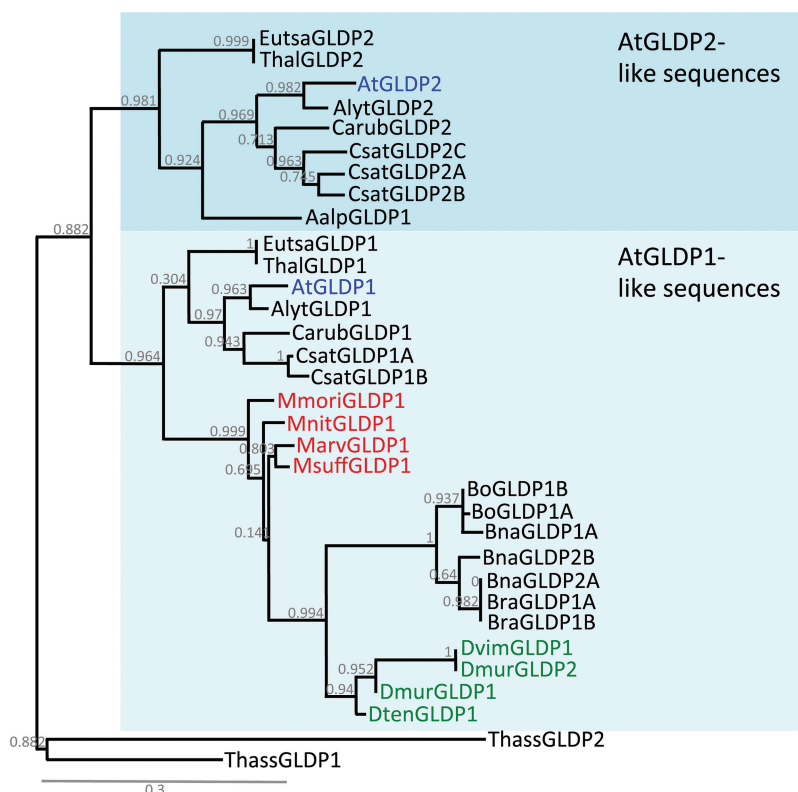
Fig. 7. Phylogenetic tree of the glycine decarboxylase P-protein (GLDP) coding sequences in selected Brassicaceae. The *GLDP* copies from *Arabidopsis thaliana* are highlighted in blue, *Moricandia* species are in red, and *Diplotaxis* species are in green. Species abbreviations are: At, *Arabidopsis thaliana*; Alyt, *Arabidopsis lyrata*; Aalp, *Arabis alpina*; Bna, *Brassica napus*; Bo, *B. oleraceae*; Bra, *B. rapa*; Eutsa, *Eutrema salsugineum*; Thal, *Thellungiella halophile*; Csat, *Camelina sativa*; Carub, *Capsella rubella*; Thass, *Tarenaya hassleriana*; Mmori, *Moricandia moricandioides*; Mnit, *Moricandia nitens*; Marv, *Moricandia arvansis* line MOR1; Msuff, *Moricandia suffruticosa*; Dvim, *Diplotaxis viminea*; Dten, *Diplotaxis tenuifolia*; Dmur, *Diplotaxis muralis*). Branch support is determined by an approximate likelihood ratio test.

copies of the *GLDP* gene: one is ubiquitously expressed in the leaf tissue (*GLDPB*), while transcripts of the other one were found exclusively in the BS (*GLDPA*). The transition from C$_3$ to C$_3$–C$_4$ photosynthesis in *Flaveria* was then realised via a gradual decrease and finally pseudogenization of the ubiquitously expressed copy and exclusive expression of the BS-specific gene (Schulze *et al.*, 2013).

Arabidopsis thaliana belongs to the lineage I of the Brassicaceae and also possesses two copies of the *GLDP* gene, *AtGLDP1* and *AtGLDP2*, and both are abundantly expressed in leaf tissue (Engel *et al.*, 2007). Orthologs of the genes were also detected in species from the same lineage and also in the extended lineage II of Brassicaceae. Only in the Brassiceae subgroup, which includes all known C$_3$–C$_4$ Brassicaceae species, was the *AtGLDP2*-like copy missing (Fig. 7). The step from C$_3$ to C$_3$–C$_4$ photosynthesis in the Brassicaceae was apparently facilitated by loss of the *GLDP2* copy. Analysis of the promoter region from the *AtGLDP1* gene revealed the presence of an MS (M-box) as well as a BS/vein (V-box) -specific element and these were highly conserved throughout the Brassicaceae family (Adwy *et al.*, 2015). Changes in the M-box of the promoter could therefore easily lead to loss of gene function in the mesophyll, and without a second copy of the gene, BS-specific *GLDP* expression typical for the C$_3$–C$_4$ species could be realised, driven by the V-box. This scenario is supported

by the absence of the M-box but the conserved presence of the V-box in the *GLDP* promoter of the C$_3$–C$_4$ species *Moricandia nitens* (Zhang *et al.*, 2004; Adwy *et al.*, 2015). In *Flaveria*, it has been hypothesised that a gradual decrease of MS *GLDP* expression might have been crucial for the adjustment of intercellular metabolism (Schulze *et al.*, 2013). It will be interesting to investigate whether single nucleotide changes are sufficient to completely disrupt the function of the Brassicaceae M-box. So despite the differences in the order of events in *Flaveria* and *Moricandia*, in both genera BS-specific elements were present in the *GLDP* promoter sequences of C$_3$ ancestors and the transition from C$_3$ to C$_3$–C$_4$ photosynthesis could be promoted by small changes in the genome.

C$_3$–C$_4$ characteristics are stable in different Moricandia species

Moricandia species had been characterised for their specific physiological, anatomical, and biochemical properties (Bauwe and Apel, 1979; Rawsthorne *et al.*, 1988*a*, *b*; Brown and Hattersley, 1989), but direct comparisons of the results from the different laboratories could be problematic because the features investigated might vary among different accessions of the same species (Sayre and Kennedy, 1977). We therefore tested CO$_2$ compensation points and phylogenetic relationships between

one C_3 *M. moricandioides* line and eight different C_3–C_4 intermediate lines. In the phylogenetic tree, all C_3–C_4 intermediates of *Moricandia* formed a monophyletic clade, indicating that the evolution of C_3–C_4 photosynthesis probably occurred once, with subsequent speciation (Fig. 1A). The CO_2 compensation points of all the C_3–C_4 lines tested were significantly lower than in C_3 relatives and higher than in the C_4 species *G. gynandra*, but the lines did not differ amongst each other (Fig. 1B).

In the C_3–C_4 accessions *M. arvensis* line MOR1 and *M. suffruticosa*, the reduction in CO_2 compensation point was closely associated with an increase in organelle number and their centripetal arrangement in the BS cells of the mature leaf (Fig. 3). A very similar picture has been described for the C_3–C_4 species *Moricandia spinosa* (Brown and Hattersley, 1989) and *M. arvensis* (Holaday *et al.*, 1981), as well as C_3–C_4 species from other plant families (McKown and Dengler, 2007; Muhaidat *et al.*, 2011; Khoshravesh *et al.*, 2016). BS cells in the C_3–C_4 intermediates are still in direct contact with the intercellular space and CO_2 can diffuse in and out of the cell. Therefore, the efficiency of the glycine shuttle and re-fixation of the released CO_2 depends on the close arrangement of the mitochondria, where CO_2 is released, and the chloroplasts, where the carboxylation reaction of Rubisco can profit from the proximate increase in CO_2 concentration.

After establishment of the photorespiratory glycine shuttle, further fitness gains are predicted by support of the glycine shuttle by C_4 acids, which serve as carbon backbones for re-assimilation of photorespiratory ammonia (Heckmann *et al.*, 2013; Mallmann *et al.*, 2014). The majority of *Flaveria* C_3–C_4 intermediates are characterised by enhanced PEPC activity and a limited C_4 cycle (Vogan and Sage, 2011; Mallmann *et al.*, 2014). In C_3–C_4 intermediate *Moricandia* species, the PEPC activity was not changed compared to the C_3 species (Fig. 2G). Earlier measurements of PEPC activity in *M. arvensis* showed a slight two-fold increase in comparison to the C_3 species *M. foetida* (Holaday *et al.*, 1981). However, ^{14}C labelling experiments gave no further evidence for a significant contribution of C_4 acids to the photosynthetic carbon assimilation (Holaday and Chollet, 1983; Hunt *et al.*, 1987). Values for $\delta^{13}C$, which would indicate a substantial contribution of PEPC to primary CO_2 fixation, were also indistinguishable between C_3 and C_3–C_4 *Moricandia* species. In *Flaveria*, the installation of the glycine shuttle led to implementation of different degrees of the C_4 cycle, including true C_4 photosynthesis, but in the *Moricandia* species analysed similar developments were not accompanied by a substantial C_4 pathway contribution.

C_3–C_4 specific metabolism influences metabolite but not transcript patterns in Moricandia

The absence of GLD is thought to induce enhanced glycine concentration in the MS, followed by diffusion of the metabolite to the BS (Rawsthorne and Hylton, 1991). As expected, an increase in the glycine concentration was detectable in total leaf extracts from *M. arvensis* and *M. suffruticosa* (Fig. 4). Serine, as the direct product of the GLD/SHMT, reaction is most likely one of the metabolites transported back to the MS cell. Just like glycine, its steady-state pool is typically increased in C_3–C_4 intermediate leaf extracts and is characterised by a high turnover rate in the illuminated leaf (Fig. 4; Rawsthorne and Hylton, 1991). The pools of metabolites suggested to maintain N-balance (e.g. glutamate, alanine, malate) were also increased in the C_3–C_4 *Moricandia* lines when compared to the C_3 relative species; only aspartate was enhanced in just one intermediate line. A strong preference for one of the suggested shuttle mechanisms could, however, not be detected. The results tend to suggest that many shuttles contribute to the metabolic balancing between the cells (Fig. 8), and it is very well possible that further metabolites are involved.

In contrast to the metabolite patterns, a C_3–C_4-related transcript pattern could not be detected in the PCA of *Moricandia* transcriptomes. The partly random enrichment of GO-terms in the commonly up- and down-regulated transcripts also suggested that species-specific differences had a major influence on the transcript pattern. The results differed considerably from the picture obtained for comparisons of transcriptomes from C_3 and C_4 species (Brautigam *et al.*, 2011, 2014; Gowik *et al.*, 2011), which were always characterised by a very strong C_4 signature with very high abundance of all transcripts encoding the C_4 photosynthesis proteins, including *PEPC*, *PPDK*, *ME*, *NADP-MDH*, *AspAT*, and adenosine monophosphate kinase (Brautigam *et al.*, 2014). Changes in the *Moricandia* lines were on a much smaller scale, but some transcripts encoding enzymes associated with C_4 metabolism, such as *PPDK*, *PEPCK*, a plastidic *NADP-MDH*, a cytosolic *NAD-MDH*, and three copies of *AspAT*, were also enhanced in both C_3–C_4 intermediate species. The same was true for one *PEPC* copy (Supplementary Table S5).

In *Flaveria*, only *F. chorifoliae* displayed a similar level of C_3–C_4 metabolism as the *Moricandia* species tested, with no significant contribution of PEPC and the C_4 cycle. However, even this basic C_3–C_4 intermediate species showed increases in transcript abundance of *AlaAT* and *NADP-ME*, and these changes were associated with the operation of the N-balancing shuttle mechanisms. The fact that the transcript changes in the C_3–C_4 intermediate *Moricandia*s were usually moderate or small compared with true C_4 species supported the hypothesis that there was not one main shuttle operating. Not all steps predicted in the model shown in Fig. 8 were accompanied by increases in transcript levels. This might not be necessary because the required enzymes are not only present in a C_3 background (Aubry *et al.*, 2011), but also of high enough abundance. It is furthermore possible that transcripts did not change in their general abundance between C_3 and C_3–C_4 species, but that they were affected in their post-transcriptional regulation or cellular distribution instead. Overall, metabolite as well as transcript patterns indicated that the N metabolism between MS and BS was adjusted by multiple pathways.

Redox balance requires transcriptional changes

When the GLD reaction is shifted to the BS, it increases not only the release of CO_2 and NH_4 in the BS mitochondria,
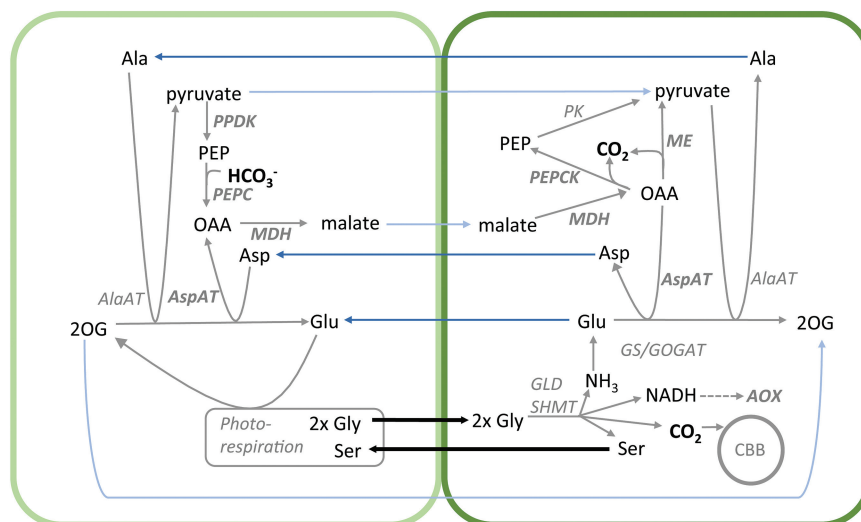
Fig. 8. Model of metabolite shuttle network active between the mesophyll cells (left) and bundle sheath cells (right) of C₃–C₄ intermediate *Moricandia* species. The inactivity of the photorespiratory glycine decarboxylating complex in the mesophyll cells leads to glycine accumulation and transport to the bundle sheath. In the mitochondria of bundle sheath cells two molecules of glycine are converted by the GLD/SHMT complex to serine, CO_2, NH_3, and NADH. In the adjacent chloroplasts the bundle sheath Rubisco is exposed to enhanced CO_2 conditions. The imbalance created by parallel release of NH_3 requires further adjustment of C and N metabolism that is probably realised by a whole network of reactions, including additional shuttling of amino acids from the bundle sheath to the mesophyll (dark blue arrows), and re-shuttling of organic acids (light blue arrows). Enzymes highlighted in bold could be associated with an increased abundance of at least one transcript copy.

but also produces high amounts of NADH (Fig. 8). In *Moricandia*, three *AOX* and one *UCP* transcripts were more abundant in the leaves of C₃–C₄ intermediate species than in the C₃ relative, suggesting that re-balancing the redox metabolism of the mitochondria is supported by alternative electron transport. Increases in *AOX* are usually found under stress, but *AOX* expression is also affected in photorespiratory mutants (Voss *et al.*, 2013). The association of enhanced alternative electron transport in C₃–C₄ photosynthesis could be verified by comparisons with the transcript patterns in different *Flaveria* species. Increases in *AOX* transcripts were also present in the intermediate species but they returned to C₃ levels in the C₄ species (Fig. 6), indicating that redox balance is harmonised again after full implementation of the C₄ cycle. This model predicts the irretrievable loss of the mitochondrial NADH transported by the photorespiratory pump.

Anatomical and environmental constrains could be responsible for impeded evolution towards C₄ in *Moricandia*

In the model presented by Mallmann *et al.* (2014), the initial shift of the GLD in the C₃–C₄ intermediates promotes a smooth transition to C₄ by gradual enhancement of the C₄ cycle, but it does not provide a straightforward explanation why some species remain stuck in intermediacy. In *Moricandia*, the analysis of potential C₄ cycle genes indicated that they are expressed, albeit at low level, in the intermediates and are theoretically capable of forming a C₄ cycle. So possible reasons for abidance of *Moricandia* in the C₃–C₄ state could be lack of time or the absence of some genetic, anatomic, or environmental drivers for the transition to C₄ to take place (Mallmann *et al.*, 2014; Heckmann, 2016).

Estimates of the time of split between C₃ and C₃–C₄ *Moricandia*s are between 11 Ma (Fig. 1A) and 2 Ma (Arias *et al.*, 2014). The same period was predicted to have passed since the separation of C₃ and C₃–C₄ intermediate *Diplotaxis* species (Fig. 1A). In *Flaveria*, one of the youngest lines evolving C₄ photosynthesis, C₃–C₄ metabolism is thought to have evolved about 3 Ma ago and, in at least one line, evolution to full C₄ photosynthesis was completed about 1–0.5 Ma ago (Christin *et al.*, 2011a). Although accurate timing of these evolutionary events is difficult, the results indicate that evolution from C₃–C₄ to C₄ might have been generally possible in the 2–11 Ma that elapsed since the origin of C₃–C₄ in *Moricandia*, but it would probably depend on several beneficial pre-conditions. Stability of C₃–C₄ metabolism for several Ma has also been described for a second lineage in *Flaveria* (*F. sonorensis*; Christin *et al.*, 2011a) and *Mollugo* (Christin *et al.*, 2011b).

Environmental conditions promoting C₄ evolution can generally be associated with conditions of high photorespiration, such as high temperatures and C limitation of photosynthesis, which can be found in hot, open environments with water limitation and high salinity (Osborne and Sack, 2012; Brautigam and Gowik, 2016). In many habitats, nutrients other than carbon, for example bio-available nitrogen or phosphorus, restrict plant growth (Korner, 2015). The low carboxylation efficiency of *Moricandia* intermediates, as indicated by low initial slopes in the A-C_i curves (Fig. 2C), point to low N-content in leaves (Sage *et al.*, 1987), probably due to reduced levels of Rubisco and CBB cycle enzymes (Fig. 5). Lower leaf N-content was supported by higher C/N ratios and lower protein content per leaf dry-weight (Fig. 2). The advantages of intermediate *Moricandia*s were thus probably limited to very low CO_2 partial pressures, as occur when stomata are closed due to water limitations, while C₃ *Moricandia*s reached higher assimilation rates under ambient CO_2, as encountered

when stomata are open. The low leaf protein content pointed to an evolutionary history of adaptation to N-limited environments. A comparison with A-C_i curves from other C_3–C_4 intermediate species showed that the phenotype is specific for *Moricandia*. In intermediate species of *Heliotropium*, the carboxylation efficiency of C_3–C_4 intermediates was slightly higher than in related C_3 species (Vogan and Sage, 2011), and the carboxylation efficiency presented for C_3–C_4 intermediate *Flaveria* species are also similar to the C_3 relatives (Dai *et al.*, 1996). Expression of CBB cycle genes was only reduced in *Flaveria* species with at least C_4-like metabolism, while transcription remained comparable to C_3 species in all C_3–C_4 intermediates (Fig. 6; Mallmann *et al.*, 2014). In both the C_3–C_4 intermediate *Moricandia* lines that were tested, on the other hand, the CBB cycle genes were already reduced at the basic intermediate state (Figs 5 and 6). Transcripts belonging to nitrogen as well as carbohydrate metabolism are enriched in the group of genes commonly reduced in the intermediate species. Thus, possibly both C and N limitation promoted the evolution of C_3–C_4 intermediacy in these species.

Finally, *Moricandia* provided new insights into the importance of anatomic enablers not only for the transition from C_3 to C_3–C_4 but also for further evolution towards C_4. Activation of BS cells and high vein density are essential pre-conditions for establishment of an efficient C_4 cycle (Christin *et al.*, 2013; Khoshravesh *et al.*, 2016). The efficiency of the glycine shuttle and connected C- and N-balancing mechanisms depend on enhanced metabolite exchange between the MS and BS cells and are therefore also dependent on a limited distance between the two cell types. The importance of the narrow vein spacing increases with the increasing contribution of a C_4 cycle in advanced C_3–C_4 intermediates and finally through to full C_4 (McKown and Dengler, 2007). Plant families in which C_4 photosynthesis evolved such as *Flaveria* and *Heliotropium* are generally characterised by vein densities considerably higher than in *Moricandia* (McKown *et al.*, 2005; Muhaidat *et al.*, 2011). It is therefore possible that limited anatomical pre-conditions hampered evolution to C_4 in the Brassiceae.

Conclusions

Current models suggest that after implementation of the photorespiratory CO_2 pump, re-balancing of N and C metabolism promotes further shuttle mechanisms involving C_4 metabolites between the MS and BS cells, and finally installation of highly efficient C_4 photosynthesis (Mallmann *et al.*, 2014; Brautigam and Gowik, 2016). In *Moricandia*, the installation of a glycine shuttle was definitely successful, and they possessed BS-specific GLDP expression, low CO_2 compensation points, and BS cells with a high number of centripetally arranged organelles. The metabolite pattern also suggests the activity of additional metabolite shuttles in the intermediates leaves. Establishment of the C_4 cycle was apparently not hampered as the C_4 cycle genes were present and expressed. Thus far, the situation in *Moricandia* does not look very different from *Flaveria*, but while some *Flaveria* lines progressed to C_4, all *Moricandia* lines remained at the basic intermediate state. Lack of progression to C_4 in the Brassicaceae

could still be connected to chance, but our *Moricandia* data now provide evidence for possible constrains on the path to C_4, namely anatomical limitation of efficient metabolite exchange or insufficient evolutionary pressure due to limitation in nutrients other than carbon, i.e. nitrogen. In contrast to C_3–C_4 lines with C_4 relatives, intermediate Brassicaeae grow in colder climates (MR Lundgren and PA Christin, unpublished data), so pressure to reduce photorespiration might also be limited. In the end, limited environmental pressure and anatomical constrains might have led to metabolic balancing by multiple pathways rather that continued promotion of the C_4 cycle in *Moricandia*. The analyses of additional intermediates with no closely related C_4 species, especially with respect to their leaf architecture and N metabolism, will hopefully provide further glimpses into the evolution of intermediacy and of C_4.

Supplementary data

Supplementary data are available at *JXB* online.

Figure S1. Phenotypes of the tested *Moricandia* lines.

Figure S2. Statistical summary of *Moricandia* metabolite patterns.

Figure S3. Statistical summary of *Moricandia* transcript patterns.

Table S1. ITS sequences extracted from the NCBI database.

Table S2. Sequences for the glycine decarboxylase P-protein.

Table S3.: Protocol for combined conventional and microwave-proceeded fixation, dehydration, and resin embedding of *Moricandia* leaf sections for histological and ultrastructural analysis.

Table S4. Summary of metabolite, element, gas exchange, anatomy, and protein measurements.

Table S5. Transcripts significantly different in abundance between the three *Moricandia* species (*M. moricandioides, M. arvensis* line MOR1 and *M. suffruticosa*)

Table S6. GO-terms enriched in commonly regulated transcripts in the comparison between C_3–C_4 and C_3 *Moricandia* species, but not different between the two C_3–C_4 *Moricandia* species.

Table S7. Changes in abundance of transcripts belonging to selected pathways.

Acknowledgements

References

Adwy W, Laxa M, Peterhansel C. 2015. A simple mechanism for the establishment of C_2-specific gene expression in Brassicaceae. The Plant Journal **84,** 1231–1238.

Apel P, Horstmann C, Pfeffer M. 1997. The Moricandia syndrome in species of the Brassicaceae – evolutionary aspects. Photosynthetica **33,** 205–215.

Arias T, Beilstein MA, Tang M, McKain MR, Pires JC. 2014. Diversification times, among Brassica (Brassicaceae) crops suggest hybrid

formation after 20 million years of divergence. American Journal of Botany **101,** 86–91.

Ashton AR, Burnell JN, Furbank RT, Jenkins CLD, Hatch MD. 1990. The enzymes in C$_4$ photosynthesis. In: Lea PJ, Harborne JB, eds. *Enzymes of primary metabolism*. London, UK: Academic Press, 39–72.

Aubry S, Brown NJ, Hibberd JM. 2011. The role of proteins in C$_3$ plants prior to their recruitment into the C$_4$ pathway. Journal of Experimantal Botany **62,** 3049–3059.

Bauwe H, Apel P. 1979. Biochemical characterization of *Moricandia arvensis* (L.) DC., a species with features intermediate between C$_3$ and C$_4$ photosynthesis, in comparison with the C$_3$ species *Moricandia foetida* Bourg. Biochemie und Physiologie der Pflanzen **174,** 251–254.

Bolger AM, Lohse M, Usadel B. 2014. Trimmomatic: a flexible trimmer for Illumina sequence data. Bioinformatics **30,** 2114–2120.

Bowes G, Ogren WL, Hageman RH. 1971. Phosphoglycolate production catalyzed by ribulose diphosphate carboxylase. Biochemical and Biophysical Research Communications **45,** 716–722.

Brautigam A, Gowik U. 2016. Photorespiration connects C$_3$ and C$_4$ photosynthesis. Journal of Experimantal Botany **67,** 2953–2962.

Brautigam A, Kajala K, Wullenweber J, *et al*. 2011. An mRNA blueprint for C$_4$ photosynthesis derived from comparative transcriptomics of closely related C$_3$ and C$_4$ species. Plant Physiology **155,** 142–156.

Brautigam A, Schliesky S, Kulahoglu C, Osborne CP, Weber AP. 2014. Towards an integrative model of C$_4$ photosynthetic subtypes: insights from comparative transcriptome analysis of NAD-ME, NADP-ME, and PEP-CK C$_4$ species. Journal of Experimantal Botany **65,** 3579–3593.

Brown RH, Hattersley PW. 1989. Leaf anatomy of C$_3$-C$_4$ species as related to evolution of C$_4$ photosynthesis. Plant Physiology **91,** 1543–1550.

Christin PA, Osborne CP, Chatelet DS, Columbus JT, Besnard G, Hodkinson TR, Garrison LM, Vorontsova MS, Edwards EJ. 2013. Anatomical enablers and the evolution of C$_4$ photosynthesis in grasses. Proceedings of the National Academy of Sciences, USA **110,** 1381–1386.

Christin PA, Osborne CP, Sage RF, Arakaki M, Edwards EJ. 2011*a*. C$_4$ eudicots are not younger than C$_4$ monocots. Journal of Experimantal Botany **62,** 3171–3181.

Christin PA, Sage TL, Edwards EJ, Ogburn RM, Khoshravesh R, Sage RF. 2011*b*. Complex evolutionary transitions and the significance of C$_3$-C$_4$ intermediate forms of photosynthesis in Molluginaceae. Evolution **65,** 643–660.

Christin PA, Spriggs E, Osborne CP, Stromberg CA, Salamin N, Edwards EJ. 2014. Molecular dating, evolutionary rates, and the age of the grasses. Systematic Biology **63,** 153–165.

Dai Z, Ku MB, Edwards GE. 1996. Oxygen sensitivity of photosynthesis and photorespiration in different photosynthetic types in the genus *Flaveria*. Planta **198,** 563–571.

Dengler NG, Dengler RE, Donnelly PM, Hattersley PW. 1994. Quantitative leaf anatomy of C$_3$ and C$_4$ grasses (Poaceae): bundle sheath and mesophyll surface area relationships. Annals of Botany **73,** 241–255.

Drummond AJ, Rambaut A. 2007. BEAST: Bayesian evolutionary analysis by sampling trees. BMC Evolutionary Biology **7,** 214.

Du Z, Zhou X, Ling Y, Zhang Z, Su Z. 2010. agriGO: a GO analysis toolkit for the agricultural community. Nucleic Acids Research **38,** W64–W70.

Edgar RC. 2004. MUSCLE: multiple sequence alignment with high accuracy and high throughput. Nucleic Acids Research **32,** 1792–1797.

Engel N, van den Daele K, Kolukisaoglu U, Morgenthal K, Weckwerth W, Parnik T, Keerberg O, Bauwe H. 2007. Deletion of glycine decarboxylase in Arabidopsis is lethal under nonphotorespiratory conditions. Plant Physiology **144,** 1328–1335.

Fiehn O, Kopka J, Dörmann P, Altmann T, Trethewey R, Willmitzer L. 2000. Metabolite profiling for plant functional genomics. Nature Biotechnology **18,** 1157–1161.

Fisher AE, McDade LA, Kiel CA, Khoshravesh R, Johnson MA, Stata M, Sage TL, Sage RF. 2015. Evolutionary history of *Blepharis* (Acanthaceae) and the origin of C$_4$ photosynthesis in section *Acanthodium*. International Journal of Plant Sciences **176,** 770–790.

Gowik U, Brautigam A, Weber KL, Weber AP, Westhoff P. 2011. Evolution of C$_4$ photosynthesis in the genus *Flaveria*: how many and which genes does it take to make C$_4$? The Plant Cell **23,** 2087–2105.

Haas BJ, Papanicolaou A, Yassour M, *et al*. 2013. *De novo* transcript sequence reconstruction from RNA-seq using the Trinity platform for reference generation and analysis. Nature Protocols **8,** 1494–1512.

Hatch MD. 1987. C$_4$ photosynthesis: a unique blend of modified biochemistry, anatomy and ultrastructure. Biochimica et Biophysica Acta **895,** 81–106.

Hatch MD, Slack CR. 1970. Photosynthetic CO$_2$-fixation pathways. Annual Review of Plant Biology **21,** 141–162.

Heckmann D. 2016. C$_4$ photosynthesis evolution: the conditional Mt. Fuji. Current Opinion in Plant Biology **31,** 149–154.

Heckmann D, Schulze S, Denton A, Gowik U, Westhoff P, Weber AP, Lercher MJ. 2013. Predicting C$_4$ photosynthesis evolution: modular, individually adaptive steps on a Mount Fuji fitness landscape. Cell **153,** 1579–1588.

Holaday AS, Chollet R. 1983. Photosynthetic/photorespiratory carbon metabolism in the C$_3$-C$_4$ intermediate species, *Moricandia arvensis* and *Panucum milioides*. Plant Physiology **73,** 740–745.

Holaday AS, Harrison AT, Chollet R. 1982. Photosynthetic/photorespiratory CO$_2$ exchange characteristics of the C$_3$-C$_4$ intermediate species, *Moricandia arvensis*. Plant Science Letters **27,** 181–189.

Holaday AS, Shien Y-J, Lee KW, Chollet R. 1981. Anatomical, ultrastructural and enzymatic studies of leaves of *Moricandia arvensis*, a C$_3$-C$_4$ intermediate species. Biochimica et Biophysica Acta **637,** 334–341.

Holbrook GP, Jordan DB, Chollet R. 1985. Reduced apparent photorespiration by the C$_3$-C$_4$ intermediate species, *Moricandia arvensis* and *Panicum milioides*. Plant Physiology **77,** 578–583.

Hunt S, Smith AM, Woolhouse HW. 1987. Evidence for a light-dependent system for reassimilation of photorespiratory CO$_2$, which does not include a C$_4$ cycle, in the C$_3$-C$_4$ intermediate species *Moricandia arvensis*. Planta **171,** 227–234.

Hylton CM, Rawsthorne S, Smith AM, Jones DA, Woolhouse HW. 1988. Glycine decarboxylase is confined to the bundle-sheath cells of leaves of C$_3$-C$_4$ intermediate species. Planta **175,** 452–459.

Kennedy RA, Laetsch WM. 1974. Plant species intermediate for C$_3$, C$_4$ photosynthesis. Science **184,** 1087–1089.

Kent WJ. 2002. BLAT—the BLAST-like alignment tool. Genome Research **12,** 656–664.

Khoshravesh R, Stinson CR, Stata M, Busch FA, Sage RF, Ludwig M, Sage TL. 2016. C$_3$-C$_4$ intermediacy in grasses: organelle enrichment and distribution, glycine decarboxylase expression, and the rise of C$_2$ photosynthesis. Journal of Experimantal Botany **67,** 3065–3078.

Korner C. 2015. Paradigm shift in plant growth control. Current Opinion in Plant Biology **25,** 107–114.

Krenzer EGJ, Moss DN, Crookston RK. 1975. Carbon dioxide compensation points of flowering plants. Plant Physiology **56,** 194–206.

Lyu M-JA, Gowik U, Kelly S, *et al*. 2015. RNA-Seq based phylogeny recapitulates previous phylogeny of the genus *Flaveria* (Asteraceae) with some modifications. BMC Evolutionary Biology **15,** 116.

Mallmann J, Heckmann D, Bräutigam A, Lercher MJ, Weber APM, Westhoff P, Gowik U. 2014. The role of photorespiration during the evolution of C$_4$ photosynthesis in the genus *Flaveria*. eLife **3,** e02478.

McKown AD, Dengler NG. 2007. Key innovations in the evolution of kranz anatomy and C$_4$ vein pattern in *Flaveria* (Asteraceae). American Journal of Botany **94,** 382–399.

McKown AD, Moncalvo J-M, Dengler NG. 2005. Phylogeny of *Flaveria* (Asteraceae) and interference of C$_4$ photosynthesis evolution. American Journal of Botany **92,** 1911–1928.

Moore BD, Franceschi VI, Shu-Hua C, Wu J, Ku MB. 1987. Photosynthetic charcteristics of the C$_3$-C$_4$ intermediate *Parthenium hystophorus*. Plant Physiology **85,** 984–989.

Morgan CL, Turner SR, Rawsthorne S. 1993. Coordination of the cell-specific distribution of the four subunits of glycine decarboxylase and serine hydroxymethyltransferase in leaves of C$_3$–C$_4$ intermediate species from different genera. Planta **190,** 468–473.

Muhaidat R, Sage TL, Frohlich MW, Dengler NG, Sage RF. 2011. Characterization of C$_3$–C$_4$ intermediate species in the genus *Heliotropium* L. (Boraginaceae): anatomy, ultrastructure and enzyme activity. Plant, Cell & Environment **34,** 1723–1736.

O'Kane SLJ, Schaal BA, Al-Shehbaz IA. 1996. The origins of *Arabidopsis suecica* (Brassicaceae) as indicated by nuclear rDNA sequences. Systematic Botany **21,** 559–566.

Osborne CP, Sack L. 2012. Evolution of C_4 plants: a new hypothesis for an interaction of CO_2 and water relations mediated by plant hydraulics. Philosophical Transactions of the Royal Society B: Biological Sciences **367,** 583–600.

Paulus JK, Schlieper D, Groth G. 2013. Greater efficiency of photosynthetic carbon fixation due to single amino-acid substitution. Nature Communications **4,** e1038.

Rajendrudu G, Prasad JSR, Das VSR. 1986. C_3-C_4 intermediate species in *Alternathera* (Amaranthaceae). Plant Physiology **80,** 409–414.

Rawsthorne S. 1992. C_3-C_4 intermediate photosynthesis: linking physiology to gene expression. The Plant Journal **2,** 267–274.

Rawsthorne S, Hylton CM. 1991. The relatonship between post-illumination CO_2 burst and glycine metabolism in leaves of C_3 and C_3-C_4 intermediate species of *Moricandia*. Planta **186,** 122–126.

Rawsthorne S, Hylton CM, Smith AM, Woolhouse HW. 1988*a*. Distribution of photorespiratory enzymes between bundle-sheath and mesophyll cells in leaves of the C_3-C_4 intermediate species *Moricandia arvensis* (L.) DC. Planta **176,** 527–532.

Rawsthorne S, Hylton CM, Smith AM, Woolhouse HW. 1988*b*. Photorespiratory metabolism and immunogold localization of photorespiratory enzymes in leaves of C_3 and C_3-C_4 intermediate species of *Moricandia*. Planta **173,** 298–308.

Robinson MD, McCarthy DJ, Smyth GK. 2010. edgeR: a Bioconductor package for differential expression analysis of digital gene expression data. Bioinformatics **26,** 139–140.

Rylott EL, Methlaff K, Rawsthorne S. 1998. Development and environmental effects on the expression of the C_3-C_4 intermediate phenotype in *Moricandia arvensis*. Plant Physiology **118,** 1277–1284.

Sage RF. 2004. The evolution of C_4 photosynthesis. New Phytologist **161,** 341–370.

Sage RF. 2016. A portrait of the C_4 photosynthetic family on the 50th anniversary of its discovery: species number, evolutionary lineages, and Hall of Fame. Journal of Experimental Botany **67,** 4039–4056.

Sage RF, Christin PA, Edwards EJ. 2011*a*. The C_4 plant lineages of planet Earth. Journal of Experimental Botany **62,** 3155–3169.

Sage RF, Khoshravesh R, Sage TL. 2014. From proto-Kranz to C_4 Kranz: building the bridge to C_4 photosynthesis. Journal of Experimental Botany **65,** 3341–3356.

Sage RF, Pearcy RW, Seemann JR. 1987. The nitrogen use efficiency of C_3 and C_4 plants. Plant Physiology **85,** 355–359.

Sage RF, Sage TL, Kocacinar F. 2012. Photorespiration and the evolution of C_4 photosynthesis. Annual Review of Plant Biology **63,** 19–47.

Sage TL, Sage RF, Vogan PJ, Rahman B, Johnson DC, Oakley JC, Heckel MA. 2011*b*. The occurrence of C_2 photosynthesis in *Euphorbia* subgenus *Chamaesyce* (Euphorbiaceae). Journal of Experimental Botany **62,** 3183–3195.

Sayre RT, Kennedy RA. 1977. Ecotypic differences in the C_3 and C_4 photosynthetic activity in *Mollugo verticillata*, a C_3-C_4 intermediate. Planta **134,** 257–262.

Schluter U, Weber AP. 2016. The road to C_4 photosynthesis: evolution of a complex trait via intermediary states. Plant and Cell Physiology **57,** 881–889.

Schulze S, Mallmann J, Burscheidt J, Koczor M, Streubel M, Bauwe H, Gowik U, Westhoff P. 2013. Evolution of C_4 photosynthesis in the genus *Flaveria*: establishment of a photorespiratory CO_2 pump. The Plant Cell **25,** 2522–2535.

Tahir M, Watts R. 2010. *Moricandia*. In: Kole C, ed. *Wild crop relatives: genomic and breeding resources*. Heidelberg, Germany: Springer Verlag.

Ueno O. 2003. Structural and biochemical dissection of photorespiration in hybrids differing in genome constitution between *Diplotaxis tenuifolia* (C_3-C_4) and radish (C_3). Plant Physiology **132,** 1550–1559.

Ueno O. 2011. Structural and biochemical characterization of the C_3-C_4 intermediate *Brassica gravinae* and relatives, with particular reference to cellular distribution of Rubisco. Journal of Experimental Botany **62,** 5347–5355.

Ueno O, Wada Y, Wakai M, Bang SW. 2006. Evidence from photosynthetic characteristics for the hybrid origin of *Diplotaxis muralis* from a C_3-C_4 intermediate and a C_3 species. Plant Biology **8,** 253–259.

Vogan PJ, Sage RF. 2011. Water-use efficiency and nitrogen-use efficiency of C_3-C_4 intermediate species of *Flaveria* Juss. (Asteraceae). Plant, Cell & Environment **34,** 1415–1430.

von Caemmerer S. 2000. *Biochemical models of leaf photosynthesis*. Collingwood, Australia: CSIRO Publishing.

Voss I, Sunil B, Scheibe R, Raghavendra AS. 2013. Emerging concept for the role of photorespiration as an important part of abiotic stress response. Plant Biology **15,** 713–722.

Warwick SI, Sauder CA. 2005. Phylogeny of tribe Brassiceae (Brassicaceae) based on chloroplast restriction site polymorphisms and nuclear ribosomal internal transcribed spacer and chloroplast trnL intron sequences. Canadian Journal of Botany **83,** 467–483.

Wen Z, Zhang M. 2015. *Salsola laricifolia*, another C_3-C_4 intermediate species in tribe Salsoleae *s.l.* (Chenopodiaceae). Photosynthsis Research **123,** 33–43.

White TJ, Bruns T, Lee S, Taylor J. 1990. Amplification and direct sequencing of fungal ribosomal RNA genes for phylogenetics. In: Innis M, Gelfand D, Sninsky J, White T, eds. *PCR protocols: a guide to methods and applications*. San Diego, USA: Academic Press, 315–322.

Williams BP, Johnston IG, Covshoff S, Hibberd JM. 2013. Phenotypic landscape inference reveals multiple evolutionary paths to C_4 photosynthesis. eLife **2,** e00961.

Zhang C, Xu G, Huang R, Chen C, Meng J. 2004. A dominant gdcP-specific marker derived from *Moricandia nitens* used for introducing the C_3-C_4 character from *M. nitens* into *Brassica* crops. Plant Breeding **123,** 438–443.